

CHARACTERIZATION OF COAL MORPHOLOGY BY SMALL ANGLE X-RAY SCATTERING (SAXS)

Mark Foster and Klavs F. Jensen

Department of Chemical Engineering and Materials Science
University of Minnesota, Minneapolis, MN 55455

INTRODUCTION

To fully understand heterogeneous reactions involving porous substances such as coal, one must have a good picture of the pore structure. This picture must reflect characteristic dimensions of the pores, their connectedness, and the surface area available for reaction on the pore walls. While the chemical structure of the coal determines the kinetics of fluid-coal reactions at the surface, the porous structure dictates how much surface is available for reaction, and what role mass transfer will play in the overall rate of reaction.

Conventional techniques for investigating pore structure, e.g. gas adsorption and Hg porosimetry, have played important roles in providing our present understanding of this structure. However, data from these methods often lead to incomplete and contradictory conclusions. Adsorption works well when measuring surface areas of nonporous or macroporous substances with chemically homogeneous surfaces. However, porosity of size scale less than 30Å is difficult to characterize with adsorption. Chemically inhomogeneous surfaces are also difficult to study. The adsorption probe molecule may adsorb preferentially on specific sites and these sites may or may not be active sites in a fluid-solid heterogeneous reaction of interest. Mercury porosimetry also works best with macroporosity. Depending on the compressibility of the sample matrix, the lower limit of pore diameter one probes may vary from 200Å to 40Å for coals (1).

Small angle x-ray scattering (SAXS) is an attractive alternative characterization technique because, above all, it is nonintrusive. Since x-rays readily penetrate the entire sample, all pores are accessible to investigation including isolated pores, i.e. those not connected to a pore leading to the particle surface. Furthermore, SAXS can study micropores as small as 10Å in diameter as well as macropores of up to 500Å in diameter. These limits may be extended using x-ray cameras designed for studying high angles or very low angles. The most exciting characteristic of SAXS is its potential for in-situ studies where the sample structure may be continually probed as it is subjected to reaction conditions.

EXPERIMENTAL METHODS

The objectives of the present SAXS studies are 1) to measure the specific surface area of the sample and 2) to infer a pore size distribution. In pursuing these objectives three types of samples are used; a model microporous carbon, three coals, and a porous γ -alumina. The model carbon is Carbosieve-S, a pure carbon molecular sieve distributed by Supelco, Inc. The manufacturer quotes a surface area of 860 m²/g for this product, but does not specify the measurement technique. Conventional N₂ BET analysis yields a value of 1100 m²/g. The carbon's highly homogeneous microporosity has been imaged with transmission electron microscopy by Fryer (2).

Basic data on the three coal samples is summarized in Table I. The anthracite coal, with its low mineral matter content and high carbon content provides the best approximation to a true two phase system of carbon and void. Anthracite, more than lower rank coal, also has microporosity similar to that in Carbosieve. The first scattering experiments with coal were therefore performed with anthracite. The other two coals were used in a study of pore change with pyrolysis due to their higher volatile matter content.

The Carbosieve and coal samples were gasified in pure CO₂ at 825°C and 1 atm in a thermogravimetric apparatus (TGA). The proper precautions were taken to ensure

Table I. PSOC Coal Samples

Type	PSOC #	Name	% C	% Mineral
Anthracite	870	Primrose	93.05	2.90
Low Volatile Bituminous	127	Lower Kittanning	84.45	5.16
High Volatile Bituminous	980	Gentry	80.40	3.97

that this reaction proceeded without mass transfer limitations. The coal samples were slowly pyrolyzed in N_2 in the TGA at a heating rate of $8^\circ C/sec$ before beginning gasification. A pyrolysis reactor containing a heated wire mesh was used for preparing samples at higher heating rates (up to $260^\circ C/sec$) for the study of varying pyrolysis conditions.

The third type of sample studied here is a porous alumina powder provided by W.R. Grace, Davison Chemical Division. Pore distributions from both N_2 adsorption and Hg porosimetry are provided by the manufacturer. The maximum of the adsorption pore volume distribution lies at a pore radius of 32\AA , and the pore volume median radius is 41\AA . The N_2 BET surface area is $339\text{ m}^2/g$. Traditional analysis of the porosimetry data yields a radius of 35\AA for the maximum of the pore volume distribution.

SMALL ANGLE X-RAY SCATTERING

X-ray diffraction or "scattering" results from boundaries between phases of sufficiently different electron densities. The large electron density difference between carbon and void generates strong scattering. Figure 1 shows schematically how the x-rays are collimated, diffracted, and detected in the University of Minnesota's modified Kratky camera (3). This configuration allows simultaneous collection of scattering data for values of the scattering vector, h from 0.015 to 0.43, where

$$h = 4\pi\sin\theta/\lambda \quad 2\theta = \text{scattering angle}$$

The data, once corrected for sample transmission coefficient and parasitic scattering, is most profitably plotted as log intensity against $\log(h)$, as in Figure 4. Scattering from small inhomogeneities appear at large values of h .

All the data presented here were collected with the sample at room temperature. However, a high temperature sample cell, shown in Figure 2, has been designed and constructed for in-situ studies of coal gasification. A carbon sample may be gasified in the reaction chamber while x-rays directed through the boron nitride windows probe the change in pore structure.

Two quantities characteristic of the sample may be obtained from SAXS data without assuming a model of the pore geometry. The first is an estimate of the surface per unit volume and the second is the radius of gyration, R_g . The specific surface may be estimated from the behavior of the scattering curve for values of h such that

$$hd_m > 5.0 \quad 1)$$

where d_m is the minimum dimension of the inhomogeneity. The relationship between the scattering intensity in this region and the sample's specific surface is known as Porod's law (4). Invoking this relationship assumes that the boundaries between phases in the sample are sharp. In practice this calculation is difficult because accurate data are required for a sizeable range of h where condition 1) is met and the scattering intensity must be accurately measured to small angles also.

The radius of gyration, R_g , is more widely used and may be calculated by fitting the experimental curve with the Guinier approximation at the lowest angles (5). However, a meaningful R_g is found only for systems with nearly monodisperse inhomogeneities. Also, in order to relate R_g to a precise dimension (e.g. radius) of the inhomogeneities one must assume a model for their geometry. In general, it is best to regard R_g as a persistence length characteristic of the structure.

A great deal of information lies in the middle region of the scattering curve, but it is neglected by a Porod or Guinier analysis alone. When the system under study is polydisperse, the Guinier approximation should not be used. Information about sizes of the inhomogeneities may be derived from fitting the entire curve with a reasonable model of the structure. We have considered two models for analysis of SAXS curves from coal and chars, the Voronoi model (6) and the Fully Penetrable Polydisperse Spheres (FPPS) model. We believe this is the first application of FPPS to the modelling of small angle scattering. Thus this work represents an extension of the work of Chiew and Glandt (7) and Torquato and Stell (8).

The most convenient model for deriving a pore size distribution is one which assumes the pores are discrete spheres (9). Such a model is obviously not consistent with the interconnected nature of coal porosity. The geometric regularity of these models and cylindrical pore models used by engineers studying gasification is inconsistent with the irregularity of actual char structure. Both the Voronoi and FPPS models correspond to interconnected, random porous structures with irregular pore sizes and shapes.

The theoretical scattering from the Voronoi model is completely determined by the measurement of ϕ_v , the void fraction of the sample and the choice of c , the Poisson point density (6). Empirically, c may be related to an apparent R_g of the model which reflects a mean size of cells in the structure. To fit our curve one varies R_g . Though the Voronoi model contains a distribution of cell sizes, a choice of two characteristic R_g 's, one for macropores, one for micropores, becomes necessary for a bimodal porous sample (10).

The pores in coal char are so polydisperse that several Voronoi cell sizes would have to be used to represent the experimental scattering curves. However, the Voronoi model no longer seems applicable in this case, so the FPPS is used. A two-dimensional representation of one possible combination of pore sizes and shapes constructed by the FPPS model is shown in Figure 3. For a single mode in the pore size distribution the theoretical scattering from the FPPS model is completely specified by three quantities, the void fraction ϕ_v , and two parameters defining the distribution of sphere sizes. In this work we consider the Schulz distribution

$$f(r) = \frac{1}{\Gamma(b)} \left(\frac{b}{r_0}\right)^b r^{b-1} \exp\left(-\frac{br}{r_0}\right) \quad 2)$$

where r_0 is a mean sphere radius, and b is a parameter that measures the sharpness of the distribution. Chiew and Glandt (7) discuss the use of this distribution with FPPS to model the surface area of a porous medium.

Considering ϕ_v as a measurable quantity we see that two parameters, r_0 and b , are required to fit experimental data with a unimodal FPPS model, while only one parameter is required with the unimodal Voronoi model. Thus, greater flexibility in fitting the curves is obtained at the price of one new parameter. The parameters r_0 and b are determined by performing a least squares fit of the model to the data. Given the values of r_0 and b which minimize the error in approximating the curve, the total surface area, complete pore size distribution, and surface area distribution are obtained analytically (7).

RESULTS

Scattering curves for three samples of Carbosieve-S are shown in Figure 4 along with parametric fits of the Voronoi model to the data. The curve for untreated Carbosieve and the curve for the sample gasified to 16.6% conversion exhibit similar behavior. Both have distinct regions reflecting scattering from micropores and macropores. The scattering intensity attributable to a particular size of pore, d should fall off sharply for values of $hd > 5.0$. The sharp decrease in intensity for $0.015 < h < 0.025$ is therefore due to macropores and the drop-off for $h > 0.2$ is due to micropores. Consequently, two Voronoi cell sizes are required to represent curves 1 and 2. At a conversion of 80% the scattering due to macropores has become much

Table II. Voronoi Model Surface Areas: Change with Conversion

Conversion	Porosity	$R_{g,micro}$ (Å)	$R_{g,macro}$ (Å)	S(m ² /g)
0.00	0.375	4.5	250	1730
0.166	0.479	4.0	250	2080
0.30	0.563	4.0	250	1820
0.41	0.631	4.5	250	1720
0.68	0.80	5.0	-	1070
0.80	0.875	5.5	-	660

less important relative to that from the growing micropores, so only a micropore cell size is needed. The parameters used in fitting the curves and surface areas calculated from the Voronoi model are given in Table II. The surface areas attain a maximum at about 16% conversion.

The surface areas are greater than those previously reported (14). However, the earlier values were determined by Porod's law at insufficiently large angles. The present technique is more accurate and the values compare favorably with the large microporosity and surface areas reported by János and Stoeckli (15).

The effect of pyrolysis heating rates on char structure have been studied for two coals, Gentry and Lower Kittanning. Final results of that work will be presented at the meeting. Preliminary results for both coals suggest a small decrease in microporosity following pyrolysis independent of heating rate over the range studied (0.8-260°C/sec). However, samples of both coals pyrolyzed slowly at 0.8°C/sec and 5°C/sec all showed similar increases in microporosity. No change was seen in the microporosity of the fast pyrolysis samples.

Scattering data collected for the anthracite coal, PSOC 870, are shown in Figure 5. The raw coal shows a more gradual decrease in intensity at low values of h than does the Carbosieve. This reflects the presence of significantly more mesoporosity. Microporosity is present here, as indicated by the scattering persisting to high values of h , but there is no drop-off in intensity for the micropore region. A small amount of conversion seems to create a large change in the curve. However, some of this change occurs with pyrolysis. The further increase in intensity at middle values of h for the 50% conversion sample demonstrates a continued growth in mean pore size.

The FPPS model was used to fit the experimental scattering curve of our characterized porous alumina sample. Figure 6 presents the comparison of experimental and theoretical scattering curves. The FPPS approximation yields values of 15Å for r_0 , and 2 for b , which corresponds to a broad distribution. These results indicate a surface area of $350\text{ m}^2/\text{cm}^3$ particle volume) or $440\text{ m}^2/\text{g}$ compared to $339\text{ m}^2/\text{g}$ from N_2 BET analysis. Further refinement of the FPPS model allowing for noninteger values of b should improve the approximation.

DISCUSSION AND CONCLUSIONS

Changes in the porous structure with conversion are clearly evident in scattering data from both the model carbon and anthracite coal. Growth of the micropores in Carbosieve and of both micro- and mesopores in the coal is seen in the increasing intensity at intermediate values of h . Also, the intensity drop-off at high values of h moves in toward the mesopore scattering.

Scattering from microporosity lies at the highest values of h available with most SAXS cameras, but the microporosity contains the vast majority of surface area and must be followed. Equipment for obtaining data at still higher values of h would be very helpful. Another challenge in collecting data in the micropore region is the appearance of a broad, weak intensity maximum at $h = 0.25$ for some coal and vitrain samples (11,12). This feature may be caused by interactions between scat-

tering units made up of layers of aromatic ring structure (11,13). The models presented here do not account for this phenomena and it has not been observed in our samples.

The Voronoi and FPPS models are better for analyzing SAXS than traditional discrete models since they correspond to interconnected, random porous structures with irregular pore sizes and shapes. The Voronoi model can be used with the model carbon which appears to have a bimodal distribution with pore sizes closely grouped about the modes. However, the FPPS model, which allows for broad distributions, is more widely applicable. The FPPS model closely approximates the scattering from a characterized sample with polydisperse porosity. However, there is a marked difference between the pore size distributions derived from SAXS and those derived from N₂ adsorption and Hg porosimetry. This could be explained in terms of the inability of the two conventional techniques to appropriately characterize microporosity. However, more comparative studies of the techniques are needed.

REFERENCES

1. Nelson, J.R., Ph.D. Thesis, The Pennsylvania State University (1979).
2. Fryer, J.R., Characterization of Porous Solids, Proc. of Symposium, S.J. Gregg, D.S.W. Sing and H.F. Stoeckli, Eds., London: Society of Chemical Industry, 41 (1979).
3. Kaler, E.W., Ph.D. Thesis, University of Minnesota (1982).
4. Porod, F., Kolloid Zeitschrift 124, 83 (1951).
5. Guinier, A. and G. Fournet, Small-Angle Scattering of X-Rays, John Wiley and Sons, Inc., New York (1955).
6. Kaler, E.W. and S. Prager, J. Coll. Int. Sci. 86, 357 (1982).
7. Chiew, Y.C. and E.D. Glandt, J. Coll. Int. Sci. 99, 86 (1984).
8. Torquato, S. and G. Stell, J. Chem. Phys. 79, 1505 (1983).
9. Lin, J.S., R.W. Hendricks, L.S. Harris and C.S. Yust, J. Appl. Cryst. 11, 621 (1978).
10. Brumburger, H. and J. Goodisman, J. Appl. Cryst. 16, 83 (1983).
11. Kalliat, M., C.Y. Kwak and P.W. Schmidt, New Approaches in Coal Chemistry, ACS Symposium Series, 169, B.D. Blaustein, B.C. Bockrath and S. Friedman, Eds., ACS: Washington, D.C., 3 (1981).
12. Chiche, P., S. Durif and S. Pregermain, J. Chim. Phys. 60, 825 (1963).
13. Hirsch, P.B., Proc. Roy. Soc. A226, 143 (1954).
14. Foster, M.D. and K.F. Jensen, Proc. Int. Conf. Coal Science, Aug. 1983, 464 (1983).
15. Jánosí, A. and H.F. Stoeckli, Carbon 17, 465 (1979).

ACKNOWLEDGEMENT

The work was supported by DOE (DE-FG22-82PL 50806).

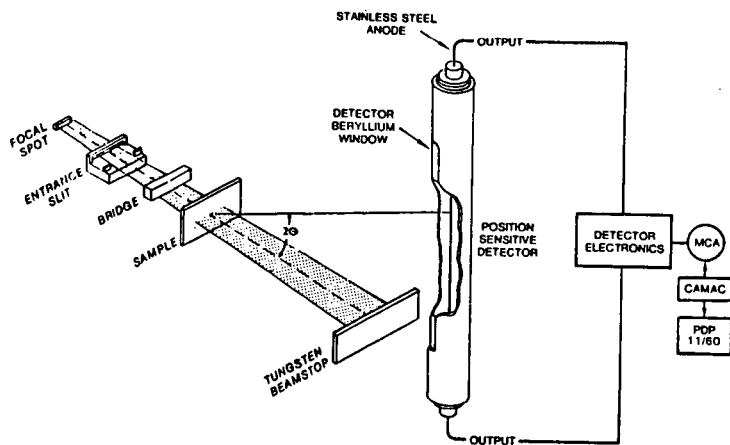
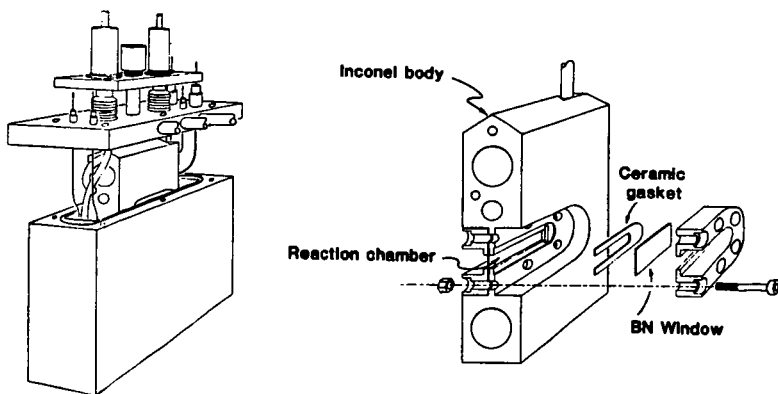


FIGURE 1. Kratky SAXS camera collimation system and detector. (From Kaler (3))



Installation in sample chamber

Cell detail: Exploded cutaway view

FIGURE 2. High temperature cell for in situ SAXS.

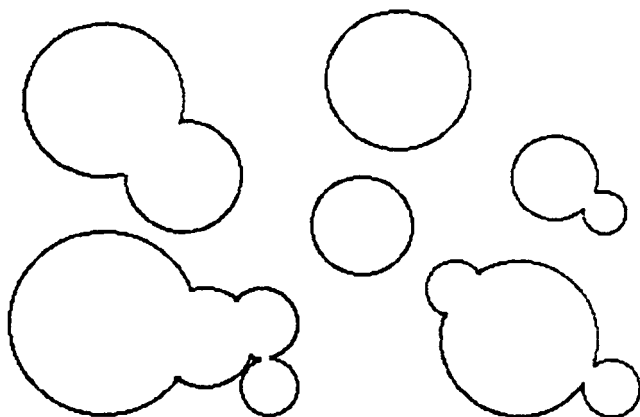


FIGURE 3. Two dimensional representation of FPPS model porous structure.

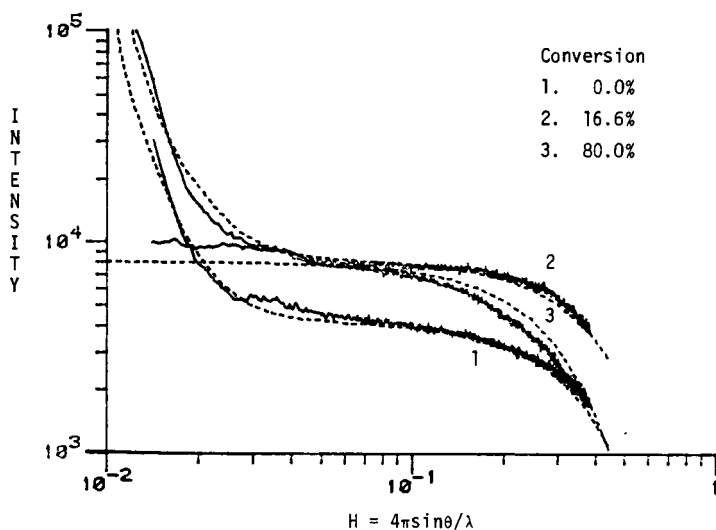


FIGURE 4. Comparison of Voronoi model approximation (----) with experimental SAXS curves (—) for Carbosieve gasified in CO_2 at 825°C .

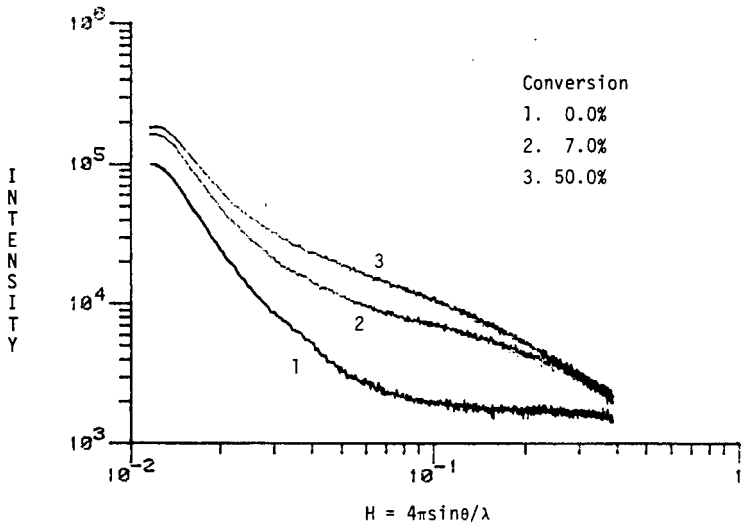


FIGURE 5. SAXS curves for Primrose anthracite (PSOC 870).

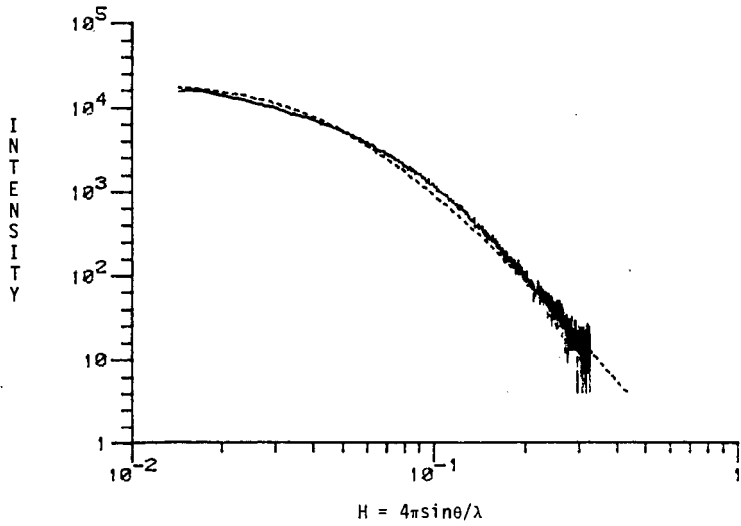


FIGURE 6. Comparison of FPPS model approximation (----) with experimental SAXS curve (—) for porous γ -alumina.